The effect of the radial electric field on neoclassical flows in a tokamak pedestal

Grigory Kagan[1], Kenneth D. Marr[2], Peter. J. Catto[2], Matt Landreman[2], Bruce Lipschultz[2] and Rachael McDermott[3]

[1]*Theoretical Division, Los Alamos National Laboratory, Los Alamos, New Mexico 87545*

[2]*Plasma Science and Fusion Center, Massachusetts Inst. of Technology, Cambridge, Massachusetts 02139*

[3]*Max-Planck-Institut für Plasmaphysik, EURATOM Association, Boltzmannstr. 2, 85748 Garching, Germany*

Abstract

Conventional formulas for neoclassical flows become inapplicable in subsonic tokamak pedestals with poloidal ion gyroradius scales since the associated strong radial electric field modifies the background ion orbits. The discrepancy has been measured to be substantial in the banana regime on Alcator C-Mod. We demonstrate that new expressions for the poloidal ion flow in the pedestal, that include the effect of the background electric field, are consistent with the boron impurity flow measurements in Alcator C-Mod.

1 Introduction

Recent measurements of the poloidal impurity flow in the pedestal of Alcator C-Mod [1] demonstrate that conventional neoclassical theories [2--4] and experiment are in reasonable agreement for Pfirsch-Schluter plasmas, but reveal a discrepancy between the two when the background ions become less collisional. This discrepancy indicates that the net flow of bulk ions is substantially less than, or even in the opposite direction to, the conventional neoclassical result. A similar change in the background ion flow is predicted by new first-principle studies of banana [5] and plateau [6] regime pedestals, which attribute the new features to a strong radial electric field. Here we demonstrate that these new theoretical results are quantitatively consistent with the experimental observations in C-Mod.

Neoclassical theory is based on the observation that in toroidal magnetic field geometry the simple Larmor motion of confined particles is superimposed on a cyclic motion of their guiding centers [7]. The radial widths of the resultant guiding center trajectories, usually referred to as drift orbits, scale with the poloidal gyroradius defined as $\rho_{p\alpha} \equiv v_\alpha m_\alpha c \big/ Z_\alpha e B_p$, where B_p is the poloidal magnetic field and m_α, Z_α, and v_α are the mass, charge number, and the thermal velocity of a plasma species respectively, with $v_\alpha \equiv \left(2T_\alpha \big/ m_\alpha\right)^{1/2}$ and T_α being the species temperature. In most tokamaks, B_p is much smaller than the total magnetic field, B, making these drift departures from a flux surface much larger than a Larmor radius.

Conventional neoclassical calculations are essentially built upon the original thin ion orbit evaluation by Galeev and Sagdeev [7], which assumes the scale-lengths of background

quantities such as the plasma density or electrostatic potential are much larger than poloidal ion gyroradius. However, this assumption breaks down in the pedestal in many experiments. Ion drift orbits in this region are then fundamentally different from those in the core because of the presence of a strong radial electric field. In a subsonic pedestal the size of this field, E_r, can be estimated from radial ion force balance by noting that the ion confinement is electrostatic to lowest order giving

$$\frac{\partial \Phi}{\partial \psi} = -\frac{1}{Z_i e n_i}\frac{\partial p_i}{\partial \psi}, \qquad (1)$$

where $E_r = -\left|\nabla \Phi\right|$ with $\Phi \cong \Phi\left(\psi\right)$ being the electrostatic potential, ψ the poloidal flux function, and n_i and $p_i = n_i T_i$ the ion density and pressure respectively [8]. Using (1), and taking the characteristic scale of the pedestal to be ρ_{pi}, the magnitude of the inward radial electric field is estimated to be

$$E_r \sim \frac{T_i}{Ze\rho_{pi}}. \qquad (2)$$

To obtain (2) the tokamak magnetic field is written as $\vec{B} = I\nabla\zeta + \nabla\zeta \times \nabla\psi$, where ζ is the toroidal angle and $I = RB_t$, with R and B_t being the major radius and the toroidal magnetic field respectively.

From (2), the variations of electrostatic and kinetic energies over a collisionless ion drift orbit are comparable. Therefore, the orbit results of Refs. [2--4,7] can no longer be utilized when developing a neoclassical theory of a banana or plateau regime pedestal, making this theory substantially different from its core counterpart. On the other hand, Pfirsch-Schluter (PS) regime

results are unaffected since the ions collide before drifting by ρ_{pi}. Accordingly, in the next section we summarize novel features of neoclassical flows discovered in the recent banana [5] and plateau [6] regime studies accounting for the electric field effect on the ion drift orbits. Then, after briefly describing in section 3 the experimental technique used to obtain the impurity flow data [1] and the radial electric field [9], in section 4 we compare this data with analytical results of Refs. [5,6]. In the last section we discuss the main factors that may affect the accuracy of the analysis and comment on a further consequence of the pedestal modification of the bulk ion flow.

2 Pedestal Theory Results

Reexamination of banana [5] and plateau [6] regime model predictions in the pedestal shows that ion heat flux and poloidal flow, as well as the neoclassical polarization and the zonal flow [10,11], are substantially modified compared to their core counterparts. In particular, it has been pointed out that the modifications to the background ion flow [5] are of the correct sign required to explain the discrepancy between the impurity flow measurements in Alcator C-Mod [1] and conventional neoclassical results [2--4,7]. A quantitative comparison between the experimental data [1] and the pedestal-relevant neoclassical results [5,6] is then presented here to demonstrate substantial agreement.

The boron impurities used in the C-Mod experiments are highly collisional so the motion of their guiding centers is unaffected by the strong background electric field. Thus, it is only their friction with the background ions that is changed in the pedestal and to leading order the usual relation [4,12--14] between the impurity and background ion flows persists. Moreover, the

results of [5,6] are asymptotic in nature since they are obtained by taking the inverse aspect ratio, ε, as small, an assumption that is only marginally true in the pedestal. Thus, consistency requires that we only retain terms to leading order in $\sqrt{\varepsilon}$ when writing the relation between the impurity and background ion flows to find

$$V_z^{pol} = V_i^{pol} - \frac{cIB_p}{e\left\langle B^2\right\rangle}\left(\frac{1}{n_i}\frac{dp_i}{d\psi} - \frac{1}{Z_z n_z}\frac{dp_z}{d\psi}\right), \tag{3}$$

where V_i^{pol}, V_z^{pol}, p_i, p_z and n_i, n_z stand for the poloidal flow, pressure and density of background ($Z_i = 1$) and impurity ions respectively, Z_z is the impurity charge number, and $\left\langle X\right\rangle$ denotes a flux surface average of X. Equation (3) conveniently provides the impurity flow velocity once the neoclassical expression for V_i^{pol} in the pedestal is inserted.

We express pedestal flows as a function of the background electric field through the parameter U defined by

$$U \equiv \frac{cI}{v_i\sqrt{\left\langle B^2\right\rangle}}\frac{d\Phi}{d\psi}. \tag{4}$$

Then, employing the banana [5] and plateau [6] regime results for V_i^{pol} along with (3), we obtain the following expressions for the poloidal flow of impurities in the pedestal:

$$V_z^{pol}\Big|_{ban} = \frac{cIB_p}{e\left\langle B^2\right\rangle}\left(\frac{1}{Zn_z}\frac{dp_z}{d\psi} - \frac{1}{n_i}\frac{dp_i}{d\psi} + 1.17J_{ban}\left(U^2\right)\frac{dT_i}{d\psi}\right), \tag{5}$$

where

$$J_{ban}\left(U^2\right) = \left(5/2 - \sigma + U^2\right)\Big/1.17 \tag{6}$$

and

$$\sigma = \frac{\int_0^\infty dy \exp\left(-y\right)\left(y+2U^2\right)^{3/2}\left(\nu_\perp y + 2\nu_{||}U^2\right)}{\int_0^\infty dy \exp\left(-y\right)\left(y+2U^2\right)^{1/2}\left(\nu_\perp y + 2\nu_{||}U^2\right)}; \qquad (7)$$

and

$$V_z^{pol}\Big|_{plateau} = \frac{cIB_p}{e\left\langle B^2\right\rangle}\left(\frac{1}{Zn_z}\frac{dp_z}{d\psi} - \frac{1}{n_i}\frac{dp_i}{d\psi} - \frac{J_p\left(U^2\right)}{2}\frac{dT_i}{d\psi}\right), \qquad (8)$$

where

$$J_p\left(U^2\right) = \frac{1+4U^2+6U^4+12U^6}{1+2U^2+2U^4}. \qquad (9)$$

In (7), $\nu_\perp = 3(2\pi)^{1/2}\nu_{ii}[\mathrm{erf}(x)-\Psi(x)]/2x^3$ and $\nu_{||} = 3(2\pi)^{1/2}\nu_{ii}\Psi(x)/2x^3$ with $x = v/v_i$, $\nu_{ii} = 4\pi^{1/2}Z^4e^4n_i\ell n\Lambda/3m_i^{1/2}T_i^{3/2}$, $\mathrm{erf}(x) = 2\pi^{-1/2}\int_0^\infty dy\exp(-y^2)$, and $\Psi(x) = [\mathrm{erf}(x) - x\,\mathrm{erf}'(x)]/2x^2$.

The shaping functions $J_{ban}\left(U^2\right)$ and $J_p\left(U^2\right)$ are normalized to unity at $U=0$ to reproduce the conventional core results in the absence of the electric field. Importantly, they are derived within the large aspect ratio approximation, in which $\left\langle B^2\right\rangle = B^2$ to leading order. We employ $\left\langle B^2\right\rangle$ to avoid ambiguity, when applying the analytical results of Refs [5,6] to the practical case of the Alcator C-Mod pedestal, where B varies poloidally.

The electric field dependent functions $J_{ban}\left(U^2\right)$ and $J_p\left(U^2\right)$ give the difference between the conventional and pedestal expressions for the poloidal flow of background ions; i.e. to evaluate V_i^{pol} in the pedestal, conventional banana and plateau results need to be multiplied by these factors. Thus, some insight into how the electric field affects the main ion, and therefore impurity, flows can be obtained by examining the dependence of J_{ban} and J_p on U^2, as U is proportional to the electric field according to (4). In the plateau case, accounting for the electric field results in the larger prediction for the main ion flow since J_p is a growing function of U^2. The banana factor, J_{ban}, decreases as U^2 grows and becomes negative at $U \approx 1.2$. Physically, this behavior means that in the banana regime pedestal the main ion flow is in the direction opposite to its core counterpart once the radial electric field goes beyond a certain critical value. Despite the character of the shaping functions being qualitatively different in the plateau and the banana cases, the electric field effect on the main ion flow results in the impurity flow becoming larger in both regimes since J_{ban} and J_p enter (5) and (8) with different signs.

The estimate of the electric field effect on the ion orbits discussed after (2) suggests that in the banana regime it is the fattest orbits that are modified the most. On the other hand, the background ion flow is carried mainly by fast passing particles, whose orbits are thinner than those of trapped and barely passing particles by a factor of $\sqrt{\varepsilon}$. This seeming contradiction is resolved by noticing that, as in the conventional case, the momentum exchange between the fast passing and trapped/barely passing fractions plays the key role in establishing the poloidal neoclassical flow in the banana regime. In other words, even though the trapped orbits do not

contribute to the net ion flow, through collisional momentum exchange they communicate information about the electric field to the freely passing particles, whose motion, otherwise unaffected by this field, constitutes the bulk ion flow. Mathematically, this mechanism of the electric field effect on the ion flow is manifested by the parameter σ entering (6), since it originates from the momentum conserving term of the ion-ion collision operator. In section 4 we compare our predictions for the banana and plateau regime edge poloidal velocity profiles, as calculated via equations (5) and (8), with the experimental data.

3 Experimental Setup

The experimental impurity velocities, temperatures, and densities are derived from charge-exchange recombination spectroscopy (CXRS) measurements at the low-field side (LFS) midplane of Alcator C-Mod. The analysis is performed on emission from fully-stripped boron, B^{5+}, which has a rest wavelength of 494.467 nm. We restrict the data included in this study to those cases that have valid velocity and temperature measurements over most of the pedestal region. In practice, this means that only H-mode data are included and the peak structure in V_z^{pol} commonly observed near the separatrix in H-mode [9] is well defined (i.e. includes data on both sides of the velocity peak). Positive poloidal velocity indicates flow in the electron diamagnetic direction at the LFS.

The data from the CXRS diagnostic are also used to calculate the radial electric field, which is needed for the evaluation of Eq. (4) and hence, equations (5)-(9). The electric field is determined experimentally by means of the radial force balance equation

$$E_r = \frac{1}{eZ_z n_z}\frac{dp_z}{dr} + V_z^{tor}B_p - V_z^{pol}B_t, \qquad (10)$$

where V_z^{tor} is the toroidal velocity of impurities. Here, the poloidal and toroidal magnetic fields, B_p and B_t, are determined by the EFIT [15] reconstruction of the plasma and the CXRS diagnostic provides the necessary velocity, temperature, and density profiles for the B^{5+} population. Further details on the determination of the edge radial electric field profile can be found in reference [9].

No direct measurement of either T_i or n_i is available at the plasma edge. However, these values are necessary when evaluating (5) and (8). Thus, we impose the following assumptions: $T_i = T_z$ and $n_i = n_e$. We expect that T_z and T_i are well correlated due to fast equilibration [1]. The use of n_e in place of n_i in the following calculations is based on quasi-neutrality. The measurement of n_e (and T_e) in the pedestal region is performed with high spatial resolution using the edge Thomson Scattering (TS) diagnostic [16].

The TS profiles are measured at a different poloidal location from the CXRS diagnostic and must be mapped to the outer midplane using the two-step procedure detailed in section 3.2 of [1]. In the first step, an initial mapping is performed using the magnetic flux surface reconstruction tool EFIT [15]. In the second step, the resulting TS-derived profiles are then shifted radially relative to those of CXRS-derived quantities so that the T_e and T_z profiles align as well as possible. This second step is performed because the EFIT reconstruction and mapping processes are only accurate to within a few millimeters, which can be important in the 2 - 6 mm thick C-Mod pedestal. Further information on the CXRS diagnostic, including discussions on alignment considerations and neutral particle sources, can be found in Refs [1,9].

4 Comparison of measured V_z^{pol} with neoclassical predictions

As shown previously [1], when both the ions and B^{5+} are in the Pfirsch-Schluter regime at the radial location of the poloidal flow peak, then the standard neoclassical expression [17]

$$V_z^{pol}\Big|_{ps} = -1.8\frac{cIB_p}{e\langle B^2\rangle}\frac{\partial T_i}{\partial \psi}, \qquad (11)$$

does a reasonable job of predicting the velocities measured by the CXRS diagnostic on Alcator C-Mod. However, when the poloidal flow peak is located where the ions are less collsional, with B^{5+} still in the Pfirsch-Schluter regime, then the standard unmodified neoclassical result poorly represents the experimental results.

We next demonstrate that the plateau and, in particular, banana regime neoclassical formulas of section 2, which are modified from their standard form through the inclusion of the effect of the strong radial electric field on background ion orbits, are in a better agreement with the pedestal measurements than conventional neoclassical theory. Of course, the boundaries between these regimes are not precisely defined, but we utilize data that is as unambiguous as possible and define these boundaries in the standard manner by $\nu_* < 1$ (banana), $1 < \nu_* < \varepsilon^{-3/2}$ (plateau), and $\varepsilon^{-3/2} < \nu_*$ (Pfirsch-Schluter), where $\nu_* \equiv \nu_{ii} qR \big/ v_i \varepsilon^{3/2}$ with q being the safety factor. We note that the predictions of the conventional and modified neoclassical formalisms differ the most in the region around the velocity peak, where the electric field is the strongest. Also, because ν_* is evaluated for the measured data, several points are considered to be in the plateau regime, whereas practically only a limited number of shots satisfy the criteria that the

peaks of *both* the measured and predicted velocity profiles are fully contained within this narrow region of the pedestal.

Figure 1 displays some typical comparisons between measured and predicted poloidal velocities for the B^{5+} poloidal velocity peak in the Pfirsch-Schluter, plateau, and banana regime cases. The first plot in each doublet (Figures 1a, c, e) shows the best match between the electric field modified neoclassical prediction and the measured values of the poloidal impurity velocity in the region near the velocity peak. The second plot in each doublet demonstrates some of the more typical discrepancies encountered when making such comparisons; i.e. Figures 1b, d, f are included to demonstrate the offsets and discrepancies commonly observed between theoretical predictions and the measured data. These discrepancies can be in the radial location or in the magnitude of the velocity adjacent to the peak and also baseline velocity.

For comparison, the poloidal velocity predictions using the unmodified neoclassical expressions are shown as dashed lines in Figures 1c-f. The difference between the solid and dashed line profiles in Figures 1c, d, e, and f is quite clear. The effect of the pedestal electric field [5,6] dramatically improves the agreement and is large enough to explain the observed discrepancies pointed out in previous work [1]. However, as we show in Figure 1f, the E_r effect in the banana regime is not always large enough to reproduce the measured velocity profiles, while Figure 1d shows that in the plateau regime the effect is at times too large.

The maximum in the poloidal flow calculated with (5) or (8) tends to occur radially outside of the maximum in the measured flow, as seen in Figures 1e-f. This radial displacement

can be observed both in shots for which the experimental maximum flow occurs in the banana regime and in shots for which it occurs in the plateau regime. The displacement is not evident in Figures 1c-d since we have excluded shots for which the theory and experiment maxima straddle different collisionality regimes. Also, in the narrow plateau regime region, this screening process tends to exclude shots for which the maxima are radially separated. The reason the theoretical peak tends to be outward of the measured peak may be the following. The peak in measured V_{pol} tends to align radially with the peak in E_r. Recall $U \propto E_r \big/ \sqrt{T_i}$ and that we assume $T_i \approx T_z$. As T_z decreases rapidly with radius, the peak in U therefore tends to be outside of the peak in measured V_{pol}. Due to the form of (5)-(6) and (8)-(9), the predicted V_{pol} tends to peak near the maximum in U, and therefore outward of the peak in measured V_{pol}. However, theory suggests $\left| dT_i \big/ d\psi \right|$ may be substantially weaker than $\left| dT_z \big/ d\psi \right|$ [8], and so the true U peak should not be shifted as far outward relative to the E_r peak. Thus, the relative displacement of the measured and predicted maxima in V_{pol} may be a result of the assumption $T_i \approx T_z$ rather than the TS-CXRS alignment issues discussed in [1].

To compare and contrast the conventional neoclassical predictions with the new ones, which account for the effect of the electric field, we present scatter plots of the peak heights from both measured and theoretical profiles in various collisionality regimes for the available data. Figure 2 shows this comparison where, for each plot, the line of complete agreement is shown (dashed). We see, as presented before in Ref. [1], that the PS regime formalism (Figure 2a) does fairly well in predicting the magnitude of the velocity peaks for high-collisionality pedestals. Figure 2b, which shows theoretical peak heights from plateau regime profiles including and not

including the effect of the radial electric field, highlights the fact that accounting for E_r results in a slightly better match between the theory and experiment. However, while using the modified formalism places the "center of mass" of the red square distribution on Figure 2b closer to the line of complete agreement, it makes the mean deviation from this line larger as well. Also, as previously mentioned, shots with both the experimental and theoretically predicted peaks in the plateau regime, such as those presented on Figures 1c-d, are rather scarce. To accumulate a sufficient number of data points in Figure 2b we allow the theoretically predicted peak to fall slightly outside the formal plateau regime boundaries. Finally, we see in Figure 2c that the agreement between experiment and the analytical banana regime result is clearly improved by the inclusion of the E_r effects. The agreement is still not perfect, but we must remember that the uncertainty in the radial electric fields calculated from the measured profiles is typically large, of order 50% inside the electric field well and 20-30% outside [9], and offset errors of a few millimeters, perhaps due to the mismatch between T_i and T_z, are possible.

5 Discussion and summary

In summary, comparisons between the poloidal impurity flow measured in the Alcator C-Mod pedestal and the radial electric field modified neoclassical expressions [5,6] are presented. No definite conclusion can be drawn in the plateau regime, but the agreement in the banana regime is clearly improved over conventional neoclassical flow predictions [1].

The investigation conducted here is limited by the shortcomings of the theory as well as experimental errors. Of course, the theoretical banana [5] and plateau [6] expressions,

employed here to explain the C-Mod measurements, are more appropriate for the pedestal region than the standard ones, since they retain the finite radial electric field effects on the ion orbits. However, these formulas are derived under concentric circular flux surface and large aspect ratio assumptions that are only marginally applicable in a realistic pedestal. In addition, experimental inaccuracies exist due to profile alignment issues, ambiguity about the separatrix location, possible differences between the main bulk and impurity ion temperatures, and the 20-50% uncertainty associated with measuring the E_r from radial B^{5+} momentum balance.

In spite of these limitations, using the modified formula (5) instead of the conventional one noticeably improves the agreement between the banana regime measurements and theory, making it clear that the radial electric field must be accounted for when evaluating poloidal flows in a pedestal. An additional consequence of our verification of the electric field's role in modifying the impurity flow is the associated enhancement of bootstrap current in a banana regime pedestal [18]. That is, the theoretical predictions for the pedestal modifications to both the impurity flow and bootstrap current originate from the same observation that the electric field effect on ion drift orbits leads to the poloidal flow of background ions being reduced in magnitude, or even reversed, compared to its core counterpart. Hence, by presenting corroborating experimental evidence of the impurity-related implications of the theory, the quantitative analysis herein also supports the conclusion that the bootstrap current is enhanced in a banana regime pedestal.

Acknowledgements

We thank both the C-Mod Operations Team and the Plasma Science and Fusion Center

Administration Team for their support. We owe additional thanks to R. M. Churchill and J.W. Hughes for assistance with data.

This research was supported by the US Department of Energy Grants No DE-AC52-06NA25396 at the Los Alamos National Laboratory, and DE-FC02-99ER54512 and DE-FG02-91ER-54109 at the Plasma Science and Fusion Center of the Massachusetts Institute of Technology.

References

[1] K. Marr, B. Lipschultz, P. Catto, R. McDermott, M. Reinke, and A. Simakov, Plasma Phys. Controlled Fusion **52**, 055010 (2010).

[2] F. Hinton and R. Hazeltine, Reviews of Modern Physics **48**, 239 (1976).

[3] Helander P and Sigmar D J, Collisional Transport in Magnetized Plasmas (Cambridge: Cambridge University Press) (2002).

[4] S. Hirshman and D. Sigmar, Nucl. Fusion **21**, 1079 (1981).

[5] G. Kagan and P. J. Catto, Plasma Phys. Controlled Fusion **52**, 055004 and 079801 (2010).

[6] I. Pusztai and P. J. Catto, Plasma Phys. Controlled Fusion **52**, 075016 and 119801 (2010).

[7] Galeev, A. A. and Sagdeev R. Z., Sov. Phys. -JETP **26**, 233 (1968).

[8] G. Kagan and P. J. Catto, Plasma Phys. Controlled Fusion **50**, 085010 (2008).

[9] R. McDermott, B. Lipschultz, J. Hughes, P. Catto, A. Hubbard, I. Hutchinson, R. Granetz, M. Greenwald, B. LaBombard, and K. Marr, Phys. Plasmas **16**, 056103 (2009).

[10] G. Kagan and P. J. Catto, Phys. Plasmas **16**, 056105 (2009).

[11] M. Landreman and P. J. Catto, Plasma Phys. Controlled Fusion **52** 085003 (2010).

[12] Y. Kim, P. Diamond, and R. Groebner, Physics of Fluids B: Plasma Physics **3**, 2050 (1991).

[13] P. Helander, Phys. Plasmas **8**, 4700 (2001).

[14] P. J. Catto and A. N. Simakov, Phys. Plasmas **13**, 052507 (2006).

[15] L. L. Lao, J. R. Ferron, R. J. Groebner, W. Howl, H. Stjohn, E. J. Strait, and T. S. Taylor, Nucl. Fusion **30**, 1035 (1990).

[16] J. Hughes, D. Mossessian, A. Hubbard, E. Marmar, D. Johnson, and D. Simon, Rev. Sci. Instrum. **72**, 1107 (2001).

[17] R. Hazeltine, Phys. Fluids **17**, 961 (1974).

[18] G. Kagan and P. J. Catto, Phys. Rev. Lett. **105**, 45002 (2010).

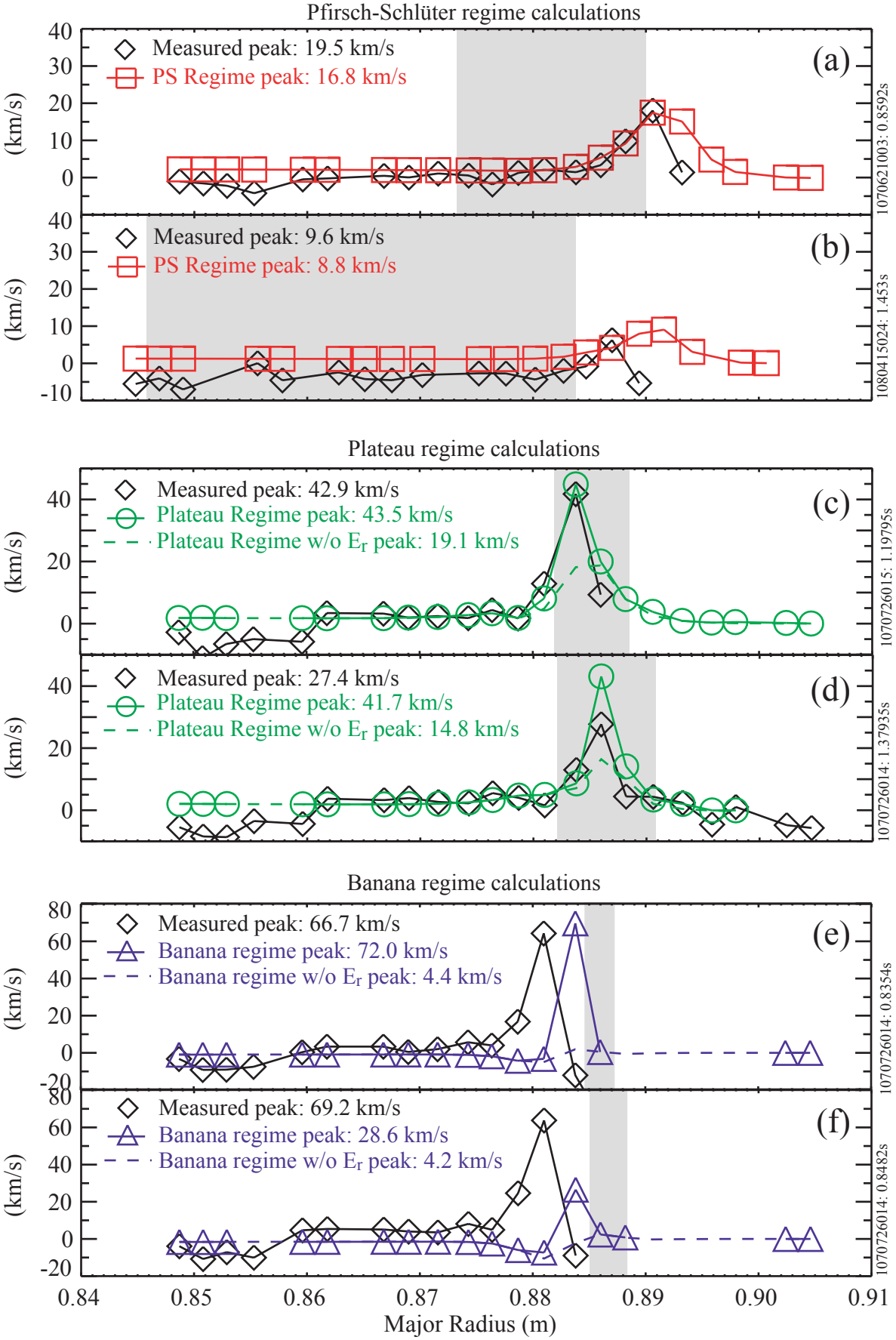

Figure 1: The comparison of measured poloidal velocity to the predictions from neoclassical theory for various collisionality plasmas: a, b) Pfirsch-Schlüter regime. c, d) Plateau regime. e, f) Banana regime. The shaded region indicates the portion of the plasma estimated to be in the plateau regime. To the left (right) of this shaded region the plasma is in the banana (Pfirsch-Schlüter) regime. Here, positive velocities indicate flow in the electron diamagnetic direction.

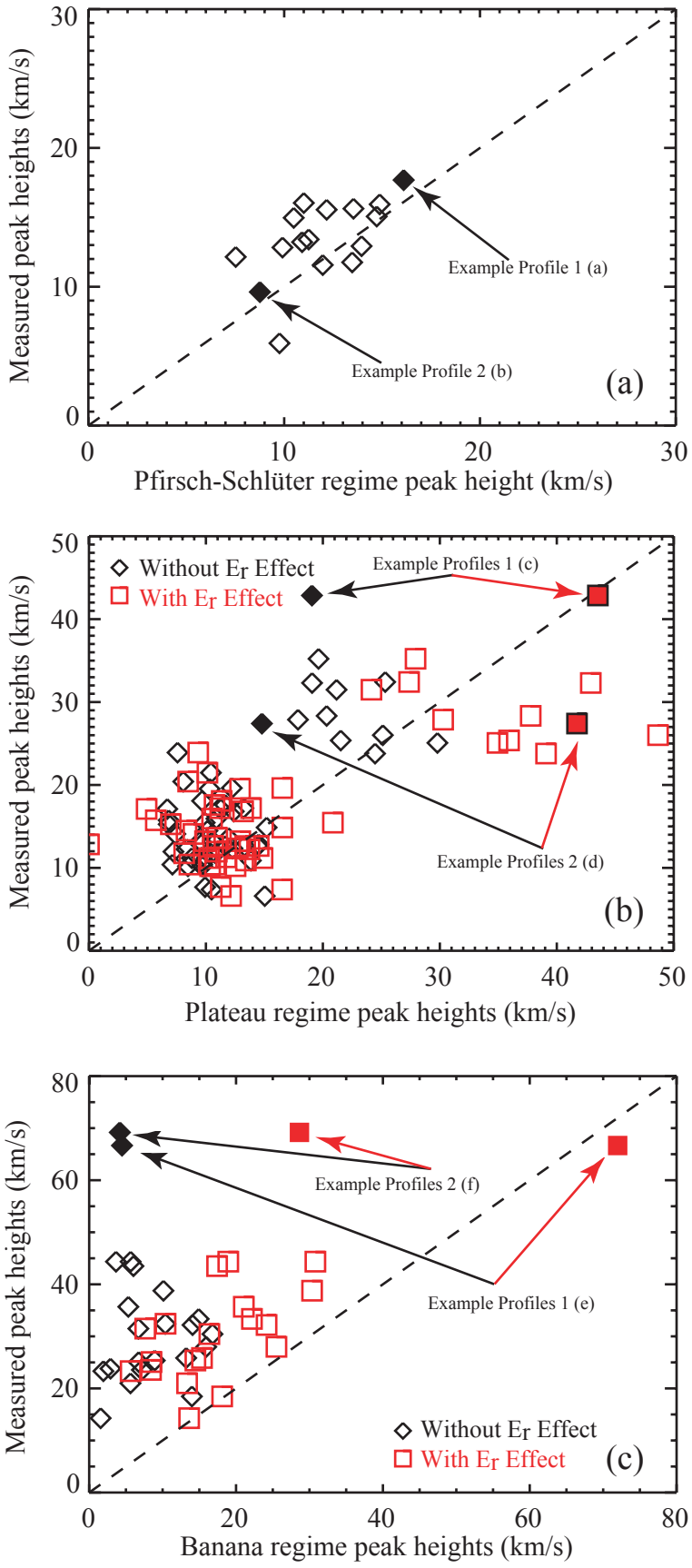

Figure 2: Comparison of predicted and experimental peak heights found near the separatrix in the poloidal velocity profile for various collisionality plasmas: a) PS regime. b) Plateau regime. c) Banana regime. Complete agreement is indicated by the dashed line. Positive velocities indicate flow in the electron diamagnetic direction. The data corresponding to the poloidal velocity profiles in Figure 1 are indicated.